Bioorganic & Medicinal Chemistry 17 (2009) 484–491

Contents lists available at ScienceDirect

Bioorganic & Medicinal Chemistry

journal homepage: www.elsevier.com/locate/bmc

Interaction between double helix DNA fragments and a new topopyrone acting as human topoisomerase I poison

Leonardo Scaglioni [a], Stefania Mazzini [a], Rosanna Mondelli [a,*], Sabrina Dallavalle [a], Sonia Gattinoni [a], Stella Tinelli [b], Giovanni L. Beretta [b], Franco Zunino [b], Enzio Ragg [a]

[a] Dipartimento di Scienze Molecolari Agroalimentari, Università di Milano, via Celoria 2, 20133 Milano, Italy
[b] Department of Experimental Oncology and Laboratories, Fondazione IRCCS Istituto Nazionale dei Tumori, via Venezian 1, 20133 Milano, Italy

ARTICLE INFO

Article history:
Received 3 October 2008
Revised 28 November 2008
Accepted 2 December 2008
Available online 10 December 2008

Keywords:
Drug-DNA interactions
NMR spectroscopy
Topopyrones
Topoisomerase I inhibitors

ABSTRACT

A water soluble derivative (**2**) of topopyrones was selected for NMR studies directed to elucidate the mode of binding with specific oligonucleotides. Topopyrone **2** can intercalate into the CG base pairs, but the residence time into the double helix is very short and a fast chemical exchange averaging occurs at room temperature between the free and bound species. The equilibria involved become slow below room temperature, thus allowing to measure a mean lifetime of the complex of ca. 7 ms at 15 °C. Structural models of the complex with $d(CGTACG)_2$ were developed on the basis of DOSY, 2D NOESY and ^{31}P NMR experiments. Topopyrone **2** presents a strong tendency to self-associate. In the presence of oligonucleotide a certain number of ligand molecules are found to externally stack to the double-helix, in addition to a small fraction of the same ligand intercalated. The external binding to the ionic surface of the phosphoribose chains may thus represents the first step of the intercalation process.

1. Introduction

Topoisomerase I (topo I) is a nuclear enzyme that catalyzes the topological changes of DNA during replication and transcription. Topo I introduces a transient single-strand break in DNA, forming a cleavable complex through a covalent link to the 3′ phosphate with a tyrosine residue, followed by religation of the broken strand. In recent years topoisomerase I inhibitors have emerged as important antineoplastic agents. Camptothecins (CPTs), the only Topo I inhibitors in clinical use, specifically inhibit the religation step via formation of a DNA-enzyme-CPT ternary complex.[1,2] Although CPT is cytotoxic in a wide range of animal tumours, its duration of action is limited, due to a rapid reversibility of the ternary complex and to the hydrolysis of the lactone to a hydroxyacid that binds to plasma proteins. In this context, there is a need for chemically stable alternative scaffolds that act as topoisomerase I inhibitors. Only a few natural topoisomerase I inhibitors have been discovered; among them the fungal metabolites bulgarein,[3] lamellarins[4] and topopyrones.[5] Topopyrones A–D (**1a–d**) (Scheme 1) were isolated from the fermentation broth of a fungus, *Phoma sp.* BAUA2861, and two of them from *Penicillium sp.* BAUA4206. They have an anthraquinone ring system linearly or angularly fused with a 1,4-pyrone moiety.[6] All these compounds showed significant cell growth inhibitory effect dependent on topoisomerase I against a panel of tumor cell lines when tested in vitro (in the range 0.7–20 μM).[5] Most recently,[7] it was reported that, in addition to stabilization of the topoisomerase I-DNA covalent binary complex, the topopyrones are strong topoisomerase II poisons.

The same anthraquinone ring system, fused with a pyrone moiety, was found in hedamycin and other related molecules, members of the pluramycin family.[8] NMR studies on hedamycin have shown that the mechanism of action is via direct interaction with DNA through intercalation of the anthrapyrantrione chromophore and alkylation of guanine in the DNA double helix by an epoxide subunit attached to the pyranone ring.[9–11]

Recently, some groups[12,13] including ourselves[14] reported the total synthesis of the members of this class of compounds. At the same time, a series of structurally related analogues of the natural topopyrone C have been synthesised in our laboratory and tested

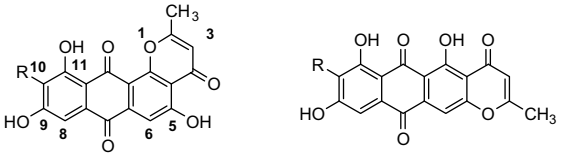

1a R = Cl Topopyrone A
1b R = H Topopyrone C
1c R = Cl Topopyrone B
1d R = H Topopyrone D

Scheme 1.

* Corresponding author. Tel.: +39 02 50316810; fax: +39 02 50316801.
E-mail address: rosanna.mondelli@unimi.it (R. Mondelli).

0968-0896/$ - see front matter © 2008 Elsevier Ltd. All rights reserved.
doi:10.1016/j.bmc.2008.12.005

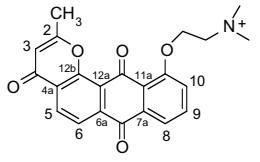

2

Scheme 2.

against human non-small cell lung cancer carcinoma NCI-H460 cell line. Most of the new analogues have shown in vitro a stronger cytotoxic activity than the parent compound (IC_{50} in the range of 4.9–7.1 μM).[15] As a part of our ongoing studies to elucidate the mechanism of action of topopyrones, a water soluble derivative (**2**) (Scheme 2), that retained a good cytotoxic activity (IC_{50} = 7.15 μM,[15] was selected for the NMR studies.

The mechanism of action of topo I inhibitors is the object of intense studies, but the role that the drug-DNA interactions play in the topo-I inhibition is still unclear. Our goal was to understand whether a direct interaction of the anthrapyrantrione ring takes place with DNA and to further characterize its mode of binding. Oligonucleotides of different sequences were used as models, that is the self-complementary duplexes $d(CGTACG)_2$, $d(CGTATACG)_2$, $d(ATGCGCAT)_2$ and $d(AAGAATTCTT)_2$.

2. Results and discussion

2.1. UV spectroscopy

As a first approach, in order to choose the best sequence for NMR study, we measured by UV spectroscopy the binding constants K of **2** on selected CG- and AT-rich oligonucleotides. By the same UV measurements we found that **2** is prone to aggregation. This is actually a common feature of many intercalating agents. A dimerization model has been considered[16,17] a sufficient approximation for the concentration range 10^{-4} to 10^{-7} M; the measured dimerization constant ($K_D = 10^5\ M^{-1}$) was thus taken into account for the numerical calculations. The apparent binding constants values are reported in Table 1. Although the binding appears in general rather weak, K values being of the order of $10^3\ M^{-1}$, the interaction for the CG-rich sequences $d(CGTACG)_2$ and $d(ATGCGCAT)_2$ seems to be preferred for the NMR studies.

2.2. NMR spectroscopy

^{1}H NMR titrations were performed on both $d(CGTACG)_2$ and $d(ATGCGCAT)_2$ by adding increasing amounts of the ligand to the oligonucleotides solution until R = [ligand]/[DNA] = 4.0 is reached. The excess of ligand enables the equilibrium to be shifted toward the formation of the complex, but the analysis of the ^{1}H NMR spectra was performed at ligand to DNA molar ratio equal to 2. This value was the best compromise between complex formation and spectral resolution. The experiments with the hexamer $d(CGTACG)_2$ gave the best results. The chemical shift variations (Table 2), observed in the ^{1}H NMR spectra of the oligonucleotide upon addition of topopyrone **2** (for R = 2), show a remarkable up-field shift for the imino and aromatic protons of C_1:G_6 and G_2:C_5 base pairs. The shielding for the imino NH G_2C_5 is the largest ($\Delta\delta$ = −0.57 ppm) and is significant because it suggests an intercalation between the base pairs at this level.

The aromatic protons of topopyrone **2** (Table 3) show similar up-field shifts. Actually, the chemical shift variation of a ligand is due to the sum of different processes, involving both specific and non-specific interactions with DNA (intercalation or minor groove binding and outside binding) and drug self-aggregation phenomena. This latter process has been proven by UV measurements (see previous section) and by NMR experiments at variable concentration (Table 3). The up-field shifts observed in the presence of DNA (R = 2) are of the same order of magnitude as those observed for the free drug at the concentration of 5.4 mM. This observation seems to indicate that the oligonucleotide favours the drug aggregation.

Table 1
Apparent binding constant values (K) for the interaction of topyrone **2** with oligonucleotides[a]

Oligonucleotide	K (M^{-1})
$d(CGTACG)_2$	4×10^3
$d(CGTATACG)_2$	1×10^3
$d(AAGAATTCTT)_2$	9×10^2
$d(ATGCGCAT)_2$	6×10^3

[a] pH 6.7, 10 mM phosphate buffer, 0.1 M NaCl, 25 °C. The values were derived from the experimental data by solving a system of non-linear equations and using MATLAB software (v. 5.1). The dimerization constant K_D (1×10^5)was included in the calculations. The standard deviation of the numerical fitting is ±20%.

Table 2
^{1}H chemical shift values for the aromatic, anomeric and imine protons of $d(CGTACG)_2$ bound to topopyrone **2**[a]

$d(CGTACG)_2$	R = 2	$\Delta\delta$
2-H A_4	7.53	−0.09
8-H A_4	8.20	−0.15
8-H G_2	7.81	−0.22
8-H G_6	7.69	−0.23
6-H C_1	7.43	−0.25
6-H T_3	7.18	−0.14
6-H C_5	7.17	−0.14
5-H C_1	5.51	**−0.42**
5-H C_5	5.15	−0.24
1′-H A_4	6.08	−0.18
1′-H G_6	5.83	−0.28
1′-H G_2	5.81	−0.20
1′-H C_1	5.51	−0.27
1′-H T_3	5.53	−0.15
1′-H C_5	5.51	−0.14
NH C_1G_6[b]	12.38	**−0.45**
NH G_2C_5	12.19	**−0.57**
NH T_3A_4	13.24	−0.28

[a] Measured in ppm at 15 °C and referenced from external DSS. Solvent D_2O, unless otherwise specified, pH 6.7, 10 mM phosphate buffer, 0.1 M NaCl. $\Delta\delta = \delta(R = 2) - \delta(R = 0)$. The complete set of values are reported in Supplementary data. All the other ribose protons are within −0.16 and 0.00 ppm.
[b] Solvent H_2O–D_2O (90:10 v/v), 5 °C.

Table 3
^{1}H chemical shift values for topyrone **2** at different concentration and in the presence of $d(CGTACG)_2$ at R = [drug]/[DNA] = 2[a]

2	R = 0 0.2 mM	R = 0 5.4 mM	$\Delta\delta$[b]	R = 2	$\Delta\delta$[c]
2-Me	2.43	2.13	−0.30	2.15	−0.28
3-H	6.35	6.00	−0.35	5.92	−0.53
5-H	8.25	7.70	−0.55	7.65	−0.60
6-H	8.02	7.54	−0.48	7.50	−0.52
8-H	7.72	7.30	−0.42	7.13	−0.59
9-H	7.75	7.48	−0.27	7.23	−0.52
10-H	7.47	7.19	−0.28	7.05	−0.42
11-OCH_2	4.53	4.30	−0.23	4.27	−0.26
NCH_2	3.73	3.60	−0.13	3.58	−0.15
NMe_2	3.08	3.02	−0.06	2.98	−0.10

[a] Measured in ppm and referenced from external DSS, solvent D_2O, 25 °C, pH 6.7, 10 mM phosphate buffer, 0.1 M NaCl.
[b] $\Delta\delta = \delta(5.4\ mM) - \delta(0.2\ mM)$.
[c] $\Delta\delta = \delta(R = 2) - \delta(R = 0$ concd 0.2 mM).

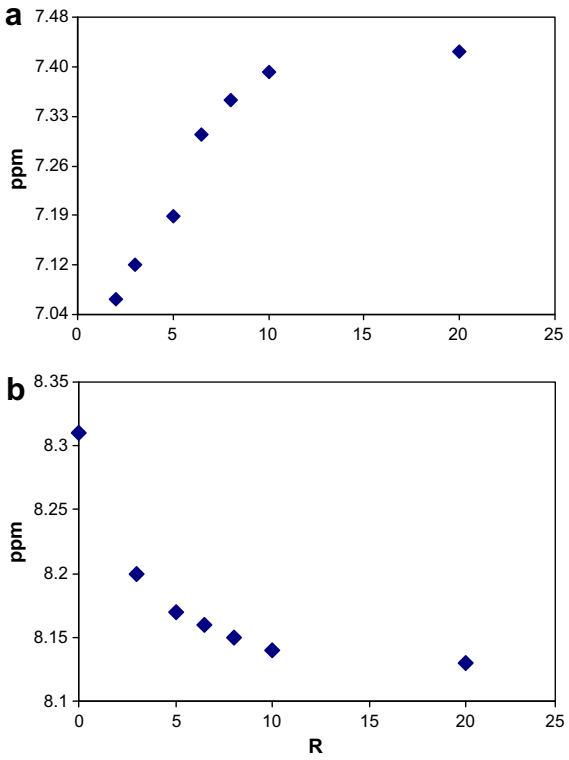

Figure 1. ^{1}H NMR chemical shift variation of (a) 10-H of topopyrone and (b) 8-H (A_4) of d(CGTACG)$_2$ as a function of the ratio R = [drug]/[DNA] in 0.1 M NaCl, 10 mM phosphate buffer, pH 6.7, 25 °C, [**2**] = 0.2 mM.

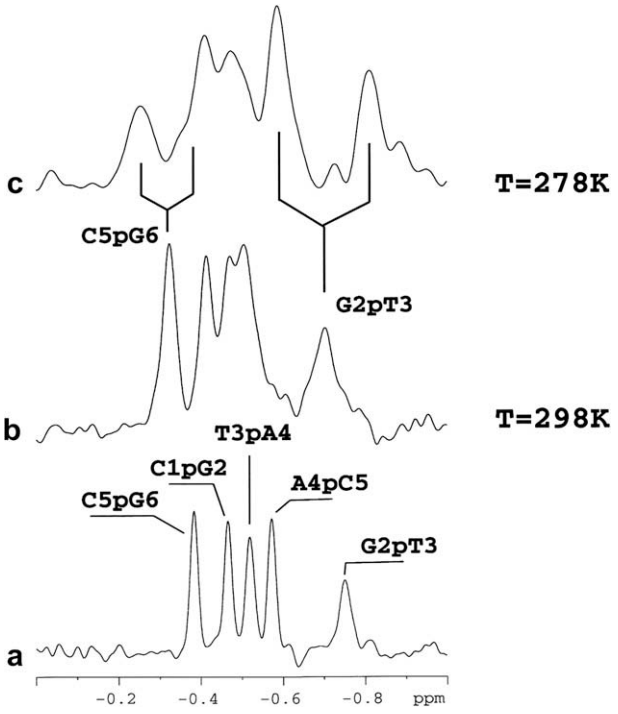

Figure 2. ^{1}H decoupled ^{31}P NMR spectra of (a) d(CGTACG)$_2$ at T = 25 °C, (b) and (c) R = [drug]/[DNA] = 1 at different temperatures.

In order to better clarify this point, the inverse titration experiment was performed, by adding increasing amounts of DNA, from R = 20 to R = 2.0, to a solution of **2** at constant concentration (0.2 mM). Figure 1 depicts the chemical shift variation observed for selected protons of the hexamer d(CGTACG)$_2$ and of topopyrone **2** during the titration experiment. In the case of topopyrone protons, Figure 1a, a stoichiometry point is reached for R values between 4 and 6. The measured chemical shift at higher R values must be related to the free drug in solution in a mixture of different aggregation states. The addition of the oligonucleotide induces a shielding of the drug protons. When an excess of oligonucleotide is reached (low values of R), the drug is found predominantly in a bound state. The shift variation curve for the nucleotide protons (Fig. 1b) confirms this finding.

The chemical shift variation of the ^{31}P resonances should provide a unique evidence of an intercalation process. A geometrical deformation in the phosphodiester chain is generally induced by changes in the DNA helical twist and is associated with a low-field shift up to 1.0–1.5 ppm, whereas a purely electrostatic association produces an up-field shift.[18] Actually, when daunomycin intercalates into d(CGTACG)$_2$ a deshielding effect of 1.3 ppm was measured[19] on C_5pG_6; while other anthracyclines of the same family, extensively studied in our laboratory,[20,21] caused a down-field shift ranging between 0.9 and 1.5 ppm. The addition of topopyrone to d(CGTACG)$_2$ until R = 2 induced a low- field shift value of 0.18 ppm for G_2pT_3, C_5pG_6 and C_1pG_2 phosphates. New ^{31}P resonances were not detected at room temperature by both 1D NMR and 2D NOESY-exchange. This indicates that the chemical equilibrium is in the fast exchange regime (on the NMR time scale), contrarily to what occurs for daunomycin at the same temperature. For R > 2 the line broadening became notable and the spectra could not be analyzed. The decrease in temperature down to 5 °C caused a further line broadening for all the resonances, but in the case of the solution with R = 1 the resonances are found to split (Figure 2). The observed splitting is due to the loss of symmetry of the double helix in the bound state, which makes the phosphate groups on the complementary strands magnetically non-equivalent. This indicates that the equilibria involved become slow at 5 °C, thus allowing the measurement of the residence time ($1/k_{off}$) at the coalescence temperature. In the case of G_2pT_3 and C_5pG_6 the coalescence temperatures were respectively 20 °C and 15 °C. Thus $1/k_{off}$ values were calculated to be respectively 4.3 ms and 6.6 ms. Such values are significantly lower than the corresponding value measured[21] for daunomycin at room temperature ($1/k_{off}$ = 20 ms).

In the present case, the small down-field effect (0.18 ppm) experienced by the phosphate groups might be at first interpreted with a small deformation in the geometry of the phosphodiester backbone (α and ζ torsion angles). However, the coexistence of external binding could mask the overall low-field shift variation, because the ionic interactions produce an up-field shift.

Due to the strong tendency of **2** to self-associate, the scheme of chemical equilibria present in solution should be much more complicated than that one depicted by a simple two-state intercalation model (free and bound species). In order to clarify the chemical equilibria present in solution and to evaluate the relevant species, several ligand/d(CGTACG)$_2$ mixtures were subjected to NMR DOSY experiments[22] The diffusion coefficient value (D) obtained for ligand **2** in the free state, $10^{-9.60}$ m^2 s^{-1}, is equivalent to a molecular weight (Mr) of 1236 Dalton and shows that its aggregation actually goes beyond dimerization, in the concentration range of NMR experiments. In the case of the complex for R = [**2**]/[DNA] = 3 the D obtained, $10^{-9.98}$ m^2 s^{-1}, is equivalent to a molecular weight of 14,970 Da; for the complex with R = 4, the D value corresponds to an Mr value of 16,206 Da (Figure 3).

The single diffusion coefficient, measured for each complex, indicates that all ligand molecules present in solution are actually bound to DNA, giving rise to a stable complex. Thus, in our experimental conditions, an outside binding of **2** with DNA occurs, in

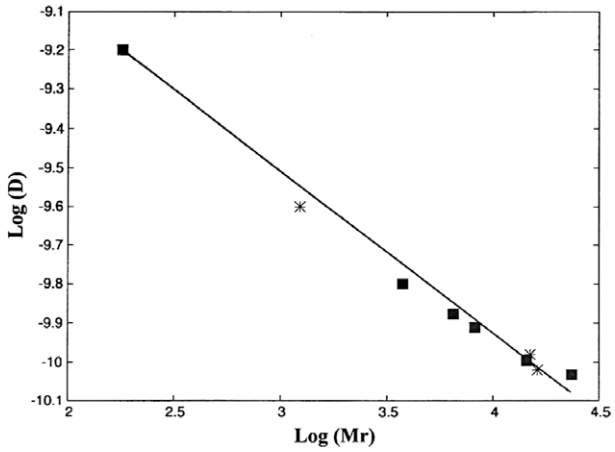

Figure 3. Molecular mass determination for the complex between topopyrone **2** and d(CGTACG)$_2$ by DOSY experiments performed at 25 °C. The calibration curve was obtained using the following standards (■): glucose (Mr 180), d(CGTACG)$_2$ (Mr 3754), aprotinin (Mr 6500), lysozyme (Mr 14400), trypsin (Mr 23500) and LCTI (Mr 7447). Diffusion coefficient values of $10^{-9.60}$ m^2 s^{-1}, $10^{-9.98}$ m^2 s^{-1} and $10^{-10.02}$ m^2 s^{-1} (*) corresponding to Mr values of 1236 Da, 14,970 Da and 16,206 Da were obtained for the ligand and complex at R = [drug]/[DNA] = 3 and 4 respectively. Correlation coefficient r^2 = 0.988.

addition to an intercalation, leading to the formation of high molecular weight aggregates, with the following molecular formula: (DNA:drug$_n$)$_3$ with n = 3–4. On this basis we built a model with three ligand molecules stacked externally to DNA. Two of them oriented with the positively charged side-chain towards the negatively charged ionic surface of the double helix and the third one with the chain in a backward orientation. A schematic representation of the molecular aggregate for $R = 4$ is reported in Figure 4.

2.3. NOESY experiments

The NOESY spectra gave a relevant number of interactions between d(CGTACG)$_2$ and the ligand (Table 4), and some examples are reported in Figure 5. Interestingly, the NOEs observed for **2**, at R = [**2**]/[DNA] = 2, are characterized by strong intensities with the same sign as those ones observed for DNA, thus indicating that both DNA and the ligand have a similar value of correlation time.[23] This observation is in line with the conclusions drawn by the DOSY experiments, that is, a single high-molecular weight aggregate is present in solution.

Specific intermolecular contacts involve 3-H, 5-H 6-H and 2-Me protons of the pyrone ring with the aromatic and ribose protons of C$_1$ and G$_2$. On the other side of the ligand molecule, the aromatic protons 9-H and 10-H of **2** showed NOE contacts with guanine G$_6$ and cytidine C$_5$. The side-chain of **2,** although flexible, showed NOE interactions at the minor groove level with 1′-H of C$_5$ and 2-H of A$_4$.

These data, especially those involving guanine G$_2$ and cytidine C$_5$ strongly suggest that an intercalation of topopyrone **2** into the terminal base pairs CG occurs, thus excluding the formation of *cap*-complexes, similar to those found for topotecan and other camptothecins.[24] Moreover, the specificity of the NOE contacts, that is, the pyrone ring with cytidine C$_1$ and guanine G$_2$, the aromatic 9,10-H protons with cytidine C$_5$ and guanine G$_6$, is not compatible with an aspecific out-side binding, where the drug molecules are externally stacked along the ionic surface of the oligonucleotide.

Actually, the ^{1}H NMR spectra at 25 °C are characterized by a fast chemical exchange regime, in analogy with the ^{31}P NMR experiments; thus, the observed ^{1}H resonances and the NOE interactions for both DNA and topopyrone **2,** in their respective free, aggregated and intercalated states, should be considered as weighted averages and the observed ligand-DNA NOEs should be interpreted as transferred-NOEs.[23] Consequently, a fraction of the same ligand is found in the intercalated state, giving rise to a relevant number of specific intermolecular ligand–DNA interactions.

A lower number of NOE interactions was extracted, due to the extensive overlapping, from the 2D-NOESY experiments performed on d(CGTATACG)$_2$ (data not shown), but the few data analyzed confirm that topopyrone prefers the terminal C:G base pairs for intercalation. In the case of d(ATGCGCAT)$_2$ the measured variation in the chemical shifts (see Supplementary data) are not very significant, being below 0.3 ppm. The extensive overlapping of all the resonances of **2** with the aromatic protons of guanines and cytidines prevented the observation of relevant intermolecular NOEs. Thus the weak NOEs detected for adenine A$_1$ and thymine T$_2$ are not sufficient to define the mode of binding. This means that d(CGTACG)$_2$ remains the best sequence for intercalation.

2.4. Molecular modeling

Driven by the experimental NOEs, several models were devised with **2** intercalated between the terminal C:G base pairs. Eight orientations were considered: four of them, with the anthrapyrone system in orthogonal position with respect to the base-pairs like daunomycins,[20] can easily be discarded, because they do not fit with the experimental NOEs; of the four orientations parallel to the bases, the two with the pyrone ring close to guanine G$_6$ and 9,10-H protons close to cytidine C$_1$ can also be discarded for the same reason. The two remaining orientations, parallel to the base pairs and with the pyrone ring close to cytidine C$_1$ and 9,10-H close to G$_6$, fit the observed NOEs and are schematically displayed as orientations A and B in Figure 6.

Two separate sets of calculations were performed with restraints in agreement with either orientation A or B (see Experimental). Figure 7 shows the obtained models for the two orientations. The inter-proton distances between ligand and oligonucleotide are reported for both complexes in Table 4. Both orientations are in good agreement with the experimental data. In orientation A, the side-chain is deeply inserted into the floor of the minor groove and anchored by Van der Waals interactions with 2-H of A$_4$ and 1′-H of C5 and by the positive edge oriented towards the negatively charged oxygen atoms of G$_6$ phosphate. The shortest

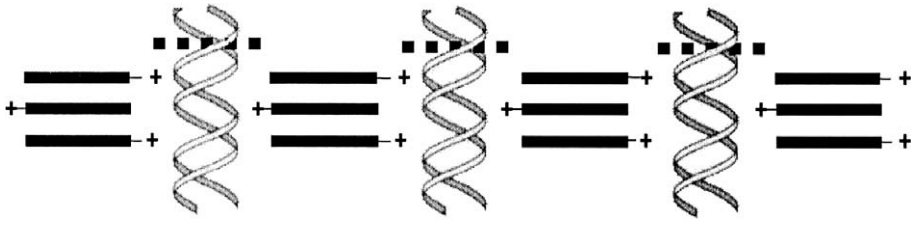

Figure 4. Scheme of the molecular aggregate for R = [drug]/[DNA] = 4. The filled and dotted black bars represent topopyrone molecules externally bound and intercalated in the double helix respectively.

Table 4
Intermolecular NOE interactions, interatomic distances (Å) and energy values for the energy minimized models (orientations A and B)

d(CGTACG)$_2$	**2**	NOE[a,b]	Distance (Å)[c]	
			A	B
6-H C_1	2-Me	s	4.8	**3.4**
8-H G_2	2-Me	m	6.0	**3.2**
6-H C_1	3-H	s	3.2	2.7
5-H C_1	3-H	s	4.5	**3.3**
1′-H C_1[d]	3-H	w	5.2	6.2
2′-H (pro*R*) C_1	3-H	s	**2.9**	6.5
2′-H (pro*S*) C_1	3-H	w	4.3	5.7
3′-H C_1	3-H	s	**2.1**	3.9
2′-H (pro*R*) G_2	3-H	s	**2.5**	4.7
2′-H (pro*S*) G_2	3-H	m	4.2	3.1
8-H G_2	5-H	m	**4.0**	5.6
5-H C_1	6-H	w	**4.1**	7.0
2′-H (pro*R*) C_1	6-H	w	7.9	**4.8**
8-H G_6	9-H	w	3.5	4.4
1′-H G_6	9-H	w	4.5	4.1
2′-H(pro*S*) G_6	9-H	s	2.2	2.7
2′-H(pro*R*) G_6	9-H	w	3.9	4.1
3′-H G_6[f]	9-H	s	2.8	2.2
1′-H C_5	9-H	s	4.4	**2.8**
2′-H(pro*S*)[e] C_5	9-H	m	3.0	3.4
5-H C_5[g]	9-H	w	5.2	6.2
8-H G_6[g]	10-H	w	5.4	**4.2**
1′-H G_6	10-H	w	4.5	5.5
2′-H(pro*R*) G_6	10-H	s	3.8	**2.7**
3′-H G_6[f]	10-H	s	3.0	3.1
1′-H C_5	10-H	s	3.0	3.2
5-H C_5[f]	10-H	m	5.2	**4.0**
Side-chain[h]				
1′-H C_5	NMe	s	**3.0**	7.6
5-H C_5	NMe	w	8.3	**3.9**
2-H A_4	NMe	s	**3.1**	8.0
1′-H A_4	NMe	w	**5.0**	10.0
Relevant conformational energy parameters *E* (Kcal/mol)				
Forcing		6.4		5.4
Van der Waals		−76.7		−83.2
Hydrogen-bond		−9.9		−8.1
Coulomb		−345		−335
Total		−239		−236
Distance violations (>0.3 Å)		1		3

[a] Acquired at 15 °C and 25 °C.
[b] *s* = 2.0–3.0 Å, *m* = 3.0–4.0 Å, *w* = 4.0–5.0 Å.
[c] The values that better define one orientation with respect to the other are in bold.
[d] Detected at *R* = 1, because the resonances of 1′-H(C_1) and 5-H(C_1) are well separated, that is, 5.61 and 5.68 ppm.
[e] 2′-H(pro*R*) of C_5 is overlapped by 2-Me of the ligand.
[f] Detected in H_2O, *R* = 1.
[g] Measured with *R* = 1.
[h] Shortest distances.

distance between the side-chain nitrogen and the oxygen atoms of C_5pG_6 phosphate is 2.9 Å. In orientation B, where the side-chain lies in the major groove, this distance is 5.3 Å.

An overview of the phosphodiester α and ζ torsion angles values, explored by both orientations during the MD simulation showed that the internal residues are found in the canonical (g^-,g^-) conformation, whereas C_1pG_2 and C_5pG_6 experience a small increase in the *trans-gauche* (t,g^-) population. In the case of orientation B, even G_2pT_3 undergoes a small shift towards the *trans-gauche* population. Therefore, the slight conformational change of these phosphates angles might explain the small down-field shift of the phosphate resonances. Some plots of the correlations between α and ζ torsion angles are reported in Figure 8.

3. Conclusion

Our NMR studies have led to the conclusion that, in addition to a stabilization of the Topo I-DNA binary cleavable complex,[15] topopyrone **2** directly interacts with the DNA double helix. The chemical equilibria present in solution are much more complicated than that depicted by a simple two-state intercalation model. In the presence of oligonucleotide a certain number of ligand molecules are found to externally stack to the double-helix, in addition to a small fraction of the same ligand that intercalates. The external binding to the ionic surface of the phosphoribose chains may thus represent the first step of the intercalation process. Due to the phosphate backbone, the polyelectrolyte behaviour of DNA facilitates the aggregation of the positively charged molecules. The external binding is then enhanced by the great tendency of topopyrone **2** to self-aggregate. The mode of binding of topopyrone **2** differs from that one observed for other topo-I inhibitors, like topotecan,[24] which prefers to stack externally to the DNA forming a *cap*-complex with the first base pairs. Topopyrone **2** is able to intercalate into the double helix between the CG base pairs. This aspect is common to daunomycins, but there is an important difference, that is, the residence time into the double helix. Daunomycin and doxorubicin have a residence time of 20 ms and 60 ms, respectively, methoxymorpholinodoxorubicin (nemorubi-

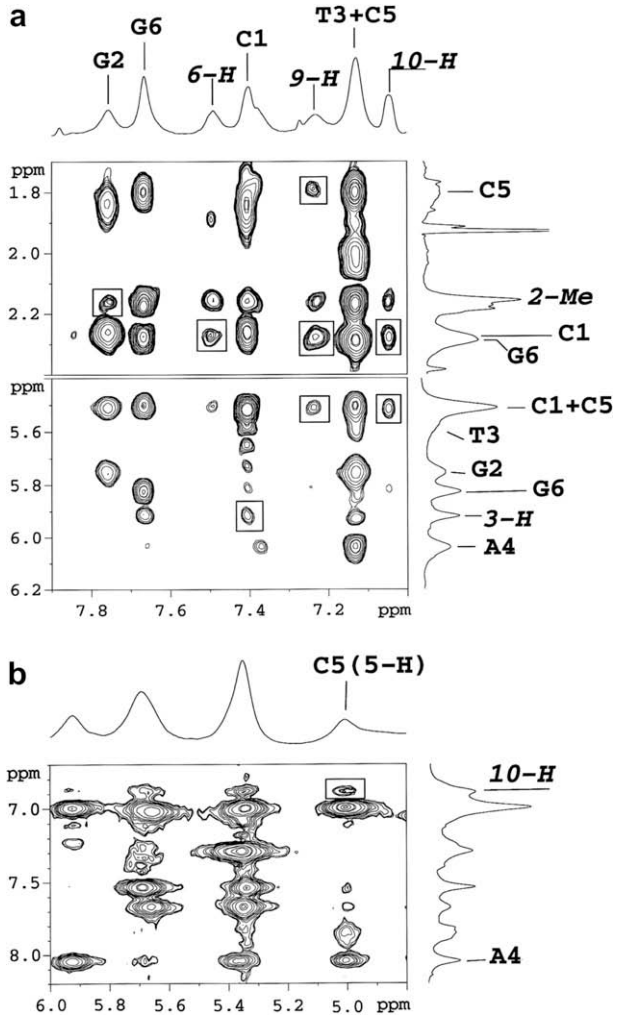

Figure 5. Selected regions of NOESY spectra of the **2**/d(CGTACG)$_2$ complex (R = 2) in (a) D_2O, (b) H_2O, phosphate buffer 10 mM pH 6.7, NaCl 100 mM, t_{mix} 300 ms, at (a) 25 °C, (b) 15 °C. The boxes show the relevant intermolecular interactions between **2** and the oligonucleotide. The protons of **2** are in italics.

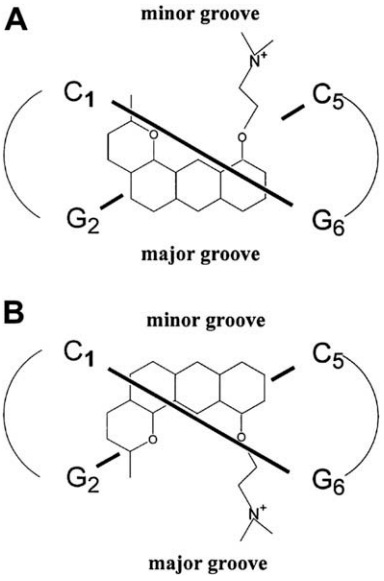

Figure 6. Schematic representation of the two different binding modes (orientations A and B) of **2** intercalated at the CpG step of d(CGTACG)$_2$.

cin), active against topo-II and topo-I,[25,26] shows the highest residence time, 450 ms, forming a very stable complex[20,21] and is strongly cytotoxic. Consequently this represents a limit for the use in therapy. Topopyrone **2** shows a residence time of 4 ms, but is still active against topo-I. In addition, the external binding to the ionic surface of the double helix might be biologically relevant and might interfere with the DNA recognition by other cellular enzymes.

The effort to find molecules less and less cytotoxic than the classical antitumour drugs is increasing in all the laboratories. On this aspect, molecules with a 'soft' binding to DNA become interesting.

The recent results[7] about the activity of topopyrones against topoisomerase II increase the interest for this class of agents.

A modulation of the binding of these molecules to DNA could be obtained by changing the side-chain with an aminosugar or a morpholino ring. The dynamic behaviour of topopyrones associated to a short residence time into the base-pairs thus appear promising.

4. Experimental

4.1. Synthesis of topopyrone *2*

Compound **2** was prepared according to the procedure previously described.[15] The synthesis was based on the use of the Marschalk alkylation reaction of the commercially available 1,8 dihydroxyanthraquinone followed by a Baker–Venkataraman chain elongation and an acid-catalyzed cyclization for the construction of the pyrone framework. The conversion of 11-hydroxy-2-methyl-1-oxabenzo[*a*]anthracene-4,7,12-trione in 11-(2-dimethylaminoethoxy)-2-methyl-1-oxabenzo[*a*]anthracene-4,7,12 trione (**2**) was achieved using (2-chloroethyl)-dimethylamine hydrochloride in tetraglyme.

4.2. Sample preparation

The oligonucleotides, purified by HPLC, were purchased from Roche Diagnostics (Monza, Italy) and dissolved in D_2O (99.9% isotopic purity, Cambridge Isotope laboratories Inc.), 0.25 mM and in H_2O/D_2O (90:10 v/v) at a 0.5–2 mM concentration range, in the presence of 0.1 M NaCl, 10 mM and 20 mM phosphate buffer, pH 6.7. For NMR titration experiments a stock solution of **2** was prepared at the concentration 23.4 mM.

7.3. NMR experiments

The NMR spectra were recorded on a Bruker AV600 spectrometer operating at a frequency of 600.10 MHz, 150.91 MHz and 242.94 MHz, for ^{1}H, ^{13}C and ^{31}P nuclei, respectively. ^{1}H and ^{31}P spectra (broad-band ^{1}H decoupled mode) were recorded at variable temperature ranging from 5 °C to 25 °C. Chemical shifts (δ) were measured in ppm. ^{1}H and ^{31}P NMR spectra were referenced respectively to external DSS (2,2-dimethyl-2-silapentane-5-sulfonate sodium salt) set at 0.00 ppm and MDA (methylenedisphosphonic acid) set at 16.8 ppm. Estimated accuracy for protons is within 0.01 ppm, for phosphorous is within 0.03 ppm. Titration experiments were performed by adding increasing amounts of **2** to a solution of the oligonucleotide (DNA), until R = [**2**]/[DNA] = 4.0 and in inverse order, by adding increasing amounts of DNA to a solution of **2** from R = 20 to R = 3.0.

Phase sensitive NOESY spectra were acquired at 25 °C and 15 °C in TPPI mode, with 2 K × 512 complex FIDs, spectral width of 8417.51 Hz and 13227.51 Hz for D_2O and H_2O solutions respectively, recycling delay of 1.5 s, 80 scans. Mixing times ranged from 50 ms to 300 ms. TOCSY[27] spectra were acquired with the use of a MLEV-17 spin-lock pulse (field strength 10.000 Hz, 60 ms total

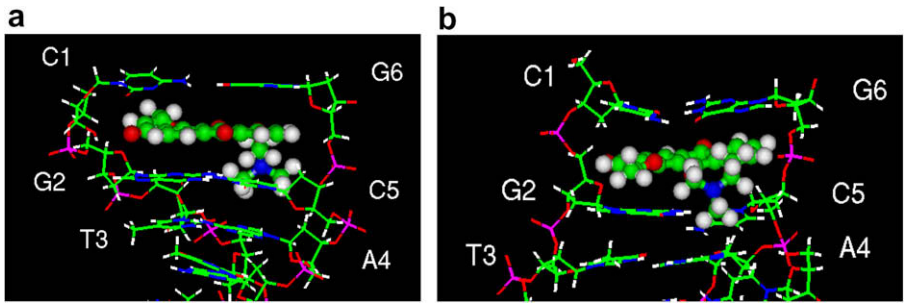

Figure 7. Energy minimized molecular models of the complex between **2** and d(CGTACG)$_2$: (a) orientation A, (b) orientation B.

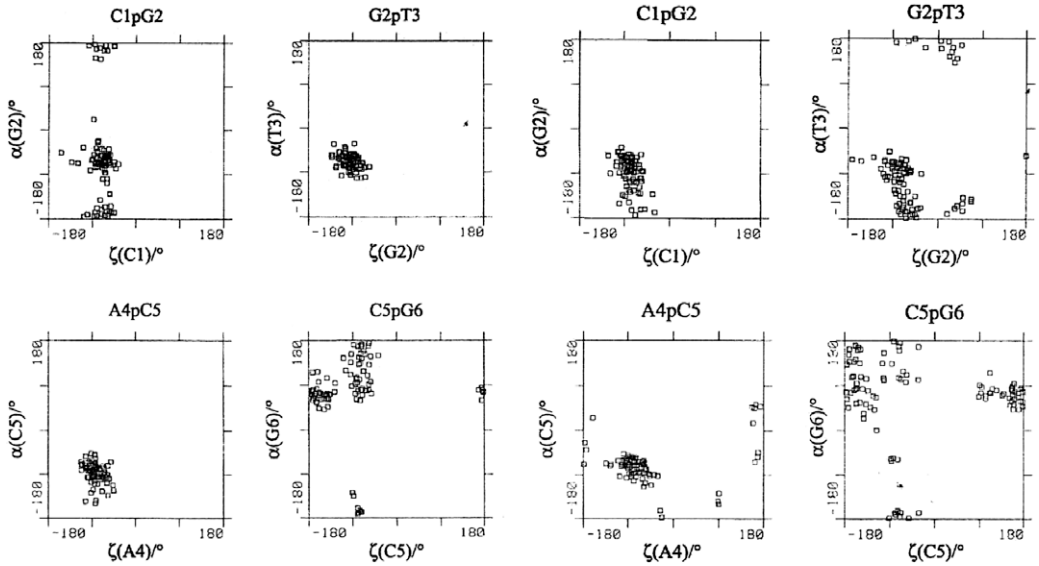

Figure 8. Correlation between torsion angles α and ζ for the C_1pG_2, G_2pT_3, A_4pC_5 and C_5pG_6 phosphate groups in the **2**/d(CGTACG)$_2$ complex obtained from MD calculations. On the left: orientation A, on the right: orientation B.

duration). All spectra were transformed and weighted with a 90° shifted sine-bell squared function to 2 K × 1 K real data points. For samples dissolved in D_2O, water suppression was achieved by pre-saturation, placing the carrier frequency on the HDO resonance. For samples in H_2O, the 3–9–19 and the excitation sculpting sequences from standard Bruker pulse program libraries were employed. ^{31}P 2D-NOESY exchange experiments were acquired (1 K × 128 FIDs, 800 scans) at different mixing times ranging from 80 to 300 ms.

^1H assignments for ligand **2** were performed by using NOESY and TOCSY experiments. The assignment of 5-H versus 6-H of **2** was made by ^{13}C HSQC and HMBC experiments. The ^{13}C assignments are reported in Supplementary data. The sequential assignments in free and bound oligonucleotides were performed by applying well established procedures for the analysis of double stranded B-DNA.[23] The assignment of 2′-H pro-*R* versus 2′-H pro-*S* for the free oligonucleodide were performed by quantification of the intra-residue NOE cross-peaks with the aromatic base protons in the NOESY spectra, in the free and bound state performed at short mixing times. The ^1H and ^{31}P assignments for the free oligonucleotides d(CGTACG)$_2$ have previously been reported,[19–21] while the ^1H assignments for d(ATGCGCAT)$_2$ with **2** are reported in Supplementary data.

Pseudo two-dimensional DOSY experiments[22] were acquired using the pulse-program 'stebpgp1s', diffusion delay: 0.12–0.45 s; gradient pulse: 1.5 ms; number of increments: 64. Raw data were processed using the standard DOSY software present in the Bruker library (TOPSPIN v. 1.3). A calibration curve was obtained using the following standards: glucose (Mr 180; 3 mM in D_2O 99.9%; NaCl 0.1 M, phosphate buffer 10 mM, pH 6.7), d(CGTACG)$_2$ (Mr 3754; 3 mM in D_2O 99.9%; NaCl 0.1 M, phosphate buffer 10 mM, pH 6.7), aprotinin (Mr 6,500; 1 mM in D_2O 99.9%; pH 6.8), lysozyme (Mr 14,400; 1 mM in D_2O 99.9%; pH 6.9), trypsin (Mr 23,500; 1 mM in D_2O 99.9%; pH 3.0) and LCTI (*Lens culinaris* trypsin inhibitor)(Mr 7447; 1 mM in D_2O 99.9%; pH 3.0).[28] The concentration of topopyrone **2** was 5.4 mM.

4.3. UV experiments

The UV spectra were recorded at 25 °C on a Perkin–Elmer Lambda 40 UV–vis spectrophotometer. Drug self-association was studied by dilution experiments measuring the change in λ_{max} of a 10^{-4} M solution diluted down to 10^{-7} M (50 mM NaCl and 10 mM phosphate buffer). A dimerization model was considered a sufficient approximation in such diluted solutions,[16,17] thus the dimerization constant (K_D) was calculated by using standard equations.[29] The apparent DNA-drug binding constants (K) were measured by titration experiments at λ_{max} of 376 nm, performed by adding increasing amounts of a 5.0×10^{-3} M stock solution of the drug in water to a 1.0×10^{-5} M solution of the oligonucleotide. An isosbestic point was observed at 414 nm. Numerical values were obtained by solving a non-linear system of equations, based on the relevant chemical equilibria present in solution, including drug self-aggregation (modeled as dimerization) and drug-DNA intercalation.[29] The numerical system was solved by using MATLAB (v.5.1).

4.4. Molecular modelling

Molecular models were built with Insight II & Discover (version 97.0 MSI, San Diego, CA) on a Silicon Graphics O2 workstation, using AMBER[30] as force-field and standard fragments from the Silicon Graphics library for **2**, partial atomic charges were calculated using MOPAC[31] and the structure energy minimized with 1000 steps conjugate gradients. For $d(CGTACG)_2$, the model was based on data taken from Ref. 24. A distance-dependent relative permittivity $\varepsilon = 4.0$ r was used and the 1–4 non bond interactions were scaled by 0.5. Initially, two different models for the intercalation (A and B) were devised by docking the ligand into DNA in the orientations suggested by the experimental NOEs. The observed NOEs were grouped into three intensity classes, corresponding to the following inter-proton distance intervals: s (strong) = 2.0–3.0 Å, m (medium) = 3.0–4.0 Å, w (weak) = 4.0–5.0 Å. Restraints were defined as quadratic well potentials with upper and lower limits on the basis of the above-reported classes of NOE intensities with a force constant of 10 Kcal mol^{-1} $Å^{-2}$. The complexes were initially subjected to energy minimization (2000 steps conjugate gradients), with the following restraints: (i) hydrogen bonds between helical base pairs (except terminal base pairs); (ii) drug-DNA interproton distances. Two separate runs were performed, after dividing the measured NOE interactions into two classes in accord to orientations A and B. As a final refinement step, a restrained molecular dynamics calculation was performed (100 ps at 300 K temperature, sampling the trajectory every ps) followed by a further minimization step.

Acknowledgments

This work was supported by the University of Milano (Funds FIRST), and MURST (Funds PRIN- 2005). Many thanks to the Dr. C. Bellucci for the calculation of *K*.

Supplementary data

Supplementary data associated with this article can be found, in the online version, at doi:10.1016/j.bmc.2008.12.005.

References and notes

1. Hsiang, Y.-H.; Hertzberg, R.; Hecht, S. M.; Liu, L. F. *J. Biol. Chem.* **1985**, *260*, 14873.
2. Thomas, C. J.; Rahier, N. J.; Hecht, S. M. *Bioorg. Med. Chem.* **2004**, *12*, 1585.
3. Fujii, N.; Yamashita, Y.; Saitoh, Y.; Nakano, H. *J. Biol. Chem.* **1993**, *268*, 13160.
4. Marco, E.; Laine, W.; Tardy, C.; Lansiaux, A.; Iwao, A.; Ishibashi, F.; Bailly, C.; Gago, F. *J. Med. Chem.* **2005**, *48*, 3796.
5. Kanai, Y.; Ishiyama, D.; Senda, H.; Iwatani, W.; Takahashi, H.; Konno, I.; Tokumasu, S.; Kanazawa, S. *J. Antibiot.* **2000**, *53*, 863.
6. Ishiyama, D.; Kanai, Y.; Senda, H.; Iwatani, W.; Takahashi, H.; Konno, I.; Kanazawa, S. *J. Antibiot.* **2000**, *53*, 873.
7. Khan, Q. A.; Elban, M. A.; Hecht, S. M. *J. Am. Chem. Soc.* **2008**, *130*, 12888.
8. Nakatani, K.; Okamoto, A.; Matsuno, T.; Saito, I. *J. Am. Chem. Soc.* **1998**, *120*, 11219.
9. Hansen, M.; Hurley, L. H. *J. Am. Chem. Soc.* **1995**, *117*, 2421.
10. Sun, D.; Hansen, M.; Hurley, L. H. *J. Am. Chem. Soc.* **1995**, *117*, 2430.
11. Owen, E. A.; Burley, G. A.; Carver, J. A.; Wickham, G.; Keniry, M. A. *Biochem. Biophys. Res. Commun.* **2002**, *290*, 1602.
12. Elban, M. A.; Hecht, S. M. *J. Org. Chem.* **2008**, *73*, 785.
13. Tan, J. S.; Ciufolini, M. A. *Org. Lett.* **2006**, *8*, 4771.
14. Gattinoni, S.; Dallavalle, S.; Merlini, L. *Tetrahedron Lett.* **2007**, *48*, 1049.
15. Dallavalle, S.; Gattinoni, S.; Merlini, L.; Mazzini, S.; Scaglioni, L.; Tinelli, S.; Beretta, G. L.; Zunino, F. *Bioorg. Med. Chem. Lett.* **2008**, *18*, 1484. and references quoted.
16. Gough, A. N.; Jones, R. L.; Wilson, W. D. *J. Med. Chem.* **1979**, *22*, 1551.
17. Charles, J. B.; Dattagupta, N.; Crothers, D. M. *Biochemistry* **1982**, *21*, 3927.
18. Gorenstein, D. J. *Chem. Rev.* **1994**, *94*, 1315.
19. Ragg, E.; Mondelli, R.; Battistini, C.; Garbesi, A.; Colonna, E. P. *FEBS Lett.* **1988**, 231.
20. Mazzini, S.; Mondelli, R.; Ragg, E. *J. Chem. Soc., Perkin Trans. 2* **1998**, 1983.
21. Bortolini, R.; Mazzini, S.; Mondelli, R.; Ragg, E.; Ulbricht, C.; Voglio, S.; Penco, S. *Appl. Magn. Reson.* **1994**, *7*, 71.
22. Morris, K. F.; Johnson, C. S., Jr. *J. Am. Chem. Soc.* **1992**, *114*, 3139.
23. Neuhaus, D.; Williamson, M. *The Nuclear Overhauser Effect in Structural and Conformational Analysis*; VCH: New York, 1998.
24. Mazzini, S.; Bellucci, M. C.; Dallavalle, S.; Fraternali, F.; Mondelli, R. *Org. Biomol. Chem.* **2004**, *2*, 505.
25. Wasserman, K.; Markovits, J.; Jaxel, C.; Capranico, G.; Kohn, K.; Pommier, Y. *Mol. Pharmacol.* **1990**, *38*, 38.
26. Zunino, F.; Pratesi, G.; Perego, P. *Biochem. Pharmacol.* **2001**, *61*, 933.
27. Bax, A.; Davis, D. G. *J. Magn. Reson.* **1985**, *65*, 355.
28. Ragg, E.; Galbusera, V.; Scarafoni, A.; Negri, A.; Tedeschi, G.; Consonni, A.; Sessa, F.; Duranti, M. *FEBS J.* **2006**, *273*, 4024.
29. Mazzini, S.; Bellucci, M. C.; Mondelli, R. *Bioorg. Med. Chem.* **2003**, *11*, 5.
30. Weiner, S. J.; Kollman, P. A.; Case, D. A.; Singh, U. C.; Ghio, C.; Alagona, G.; Profeta, S., Jr.; Weiner, P. *J. Am. Chem. Soc.* **1984**, *106*, 756.
31. Stewart, J. J. P. *J. Comput. Aided Mol. Des.* **1990**, *4*, 1.